Available online at www.sciencedirect.com

ScienceDirect

Procedia Engineering 105 (2015) 940 – 945

Procedia Engineering

www.elsevier.com/locate/procedia

6th BSME International Conference on Thermal Engineering (ICTE 2014)

Temperature Dependent Mechanical Behavior of a Locally Restrained Graphite-Aluminum Laminated Plate under Bi-axial Loading

Partha Modak, S. Reaz Ahmed*

Department of Mechanical Engineering, Bangladesh University of Engineering and Technology, Dhaka 1000, Bangladesh

Abstract

Temperature-dependent mechanical behavior of a locally restrained metal-matrix composite plate is investigated under uniform bi-axial compression. Thin rectangular plates of angle-ply and cross-ply laminate composed of Graphite-Aluminum composite are considered for the analysis. The plates are assumed to be locally restrained at their corner regions. Temperature-dependent mechanical properties of the metal-matrix composite are used in the displacement-potential analysis of the elastic response. Results of deformed shapes as well as stress distributions are demonstrated as a function of temperature and fiber-orientation of the laminate.

Peer-review under responsibility of organizing committee of the 6th BSME International Conference on Thermal Engineering (ICTE 2014)

Keywords: Mechanical behavior; Gr-Al laminate; bi-axial loading; temperature; fiber orientation; displacement potential

1. Introduction

Metal matrix composites are good candidates for aerospace applications that require a wide operating temperature range, high inter-laminar strength, and good impact resistance and lightening tolerance. While significant effort is being devoted to material development and processing, practical application of composite materials lags behind due to the lack of specific design guidance and an understanding of the material performance under actual service conditions.

Graphite fiber-reinforced aluminum composite has attracted interest of materials manufacturers and researchers [1]. Because of low thermal expansion properties and high specific stiffness, graphite-aluminum composites are leading candidates for applications in high precision space vehicles where dimensional stability in a wide temperature range is a major design criterion. The mechanical behavior of graphite fiber composites can be influenced by externally applied parameters, such as, loading, restraints, strain rate, temperature and humidity as well as fiber orientation. Recently, results of studies dealing with the characterization of graphite-aluminum composites under thermo-mechanical loading have been reported [1]. J.M. Lifshitz [2] investigated on mechanical behaviour of a graphite fiber composite under the influence of strain rate, temperature and humidity. A theoretical and experimental study of Al alloy 6061-SiC metal matrix composite was conducted to identify the operative mechanism for accelerated aging [3]. The effect

* Corresponding author. Tel.: +880-2-966-5636
E-mail address: reaz207@yahoo.com

Peer-review under responsibility of organizing committee of the 6th BSME International Conference on Thermal Engineering (ICTE 2014)
doi:10.1016/j.proeng.2015.05.119

of addition of silicon carbide filler in different weight percentages on physical, mechanical, and thermal properties of chopped glass fiber-reinforced epoxy composites has been investigated by [4]. On the other hand, the effect of fiber orientation on the mechanical behavior of structural components has now become a key subject in the field of composite structures [5,6]. A useful investigation of the effect of fiber orientation together with the exposure temperature on the stress field of Gr-Al plates is of great practical importance to define and understand the corresponding mechanical behavior and also for their improved design.

The present paper describes a new investigation of temperature dependent mechanical behavior of a metal matrix laminated plate under uniform bi-axial compression. A 45^o angle-ply and a cross-ply laminated composite of P100/6061 Gr-Al are considered for the analysis. The plates are assumed to be locally restrained at their corner regions to simulate the physical condition of tag welding. On-axis mechanical properties of the unidirectional composite obtained at different temperatures are used in the analysis. Displacement potential computational method [7,8] is used to analyze the present mixed boundary value problem of laminated composites. Results of the analysis are presented mainly in the form of deformed shape and stress distributions as a function of temperature and ply angles of the laminates.

2. Theoretical background of the analysis

The stress-strain relations for general laminated composite materials under the plane stress condition are given by [9]

$$\begin{bmatrix} \sigma_{xx} \\ \sigma_{yy} \\ \sigma_{xy} \end{bmatrix} = \frac{1}{h} \begin{bmatrix} A_{11} & A_{12} & A_{16} \\ A_{12} & A_{22} & A_{26} \\ A_{16} & A_{26} & A_{66} \end{bmatrix} \begin{bmatrix} \varepsilon_{xx} \\ \varepsilon_{yy} \\ \varepsilon_{xy} \end{bmatrix} \tag{1}$$

Here, A_{ij} are the elements of extensional stiffness matrix $[A]$ [9], which are various functions of E_1, E_2, G_{12} and ν_{12}. h is the total thickness of the laminate. With reference to a rectangular coordinate system (x, y), in absence of body forces, the two differential equations of equilibrium for the problems of symmetric laminated composites, under plane stress approximation, are as follows [9,10]:

$$A_{11}\frac{\partial^2 u_x}{\partial x^2} + 2A_{16}\frac{\partial^2 u_x}{\partial x \partial y} + A_{66}\frac{\partial^2 u_x}{\partial y^2} + A_{16}\frac{\partial^2 u_y}{\partial x^2} + (A_{12} + A_{66})\frac{\partial^2 u_y}{\partial x \partial y} + A_{26}\frac{\partial^2 u_y}{\partial y^2} = 0 \tag{2a}$$

$$A_{16}\frac{\partial^2 u_x}{\partial x^2} + (A_{12} + A_{66})\frac{\partial^2 u_x}{\partial x \partial y} + A_{26}\frac{\partial^2 u_x}{\partial y^2} + A_{66}\frac{\partial^2 u_y}{\partial x^2} + 2A_{26}\frac{\partial^2 u_y}{\partial x \partial y} + A_{22}\frac{\partial^2 u_y}{\partial y^2} = 0 \tag{2b}$$

For a symmetric laminated composite, the mid-plane strains are considered to be the global strains, as the curvature effect under in-plane loading can be neglected [9]. Moreover, for a symmetric laminate with even number of plies, A_{16} and A_{26} are zero. In the displacement-potential lamination theory, a potential function $\psi(x, y)$ is introduced in terms of the displacement components of plane elasticity, as follows:

$$\begin{bmatrix} u_x \\ u_y \end{bmatrix} = \begin{bmatrix} m_1 & m_2 & m_3 \\ n_1 & n_2 & n_3 \end{bmatrix} \begin{bmatrix} \frac{\partial^2 \psi}{\partial x^2} & \frac{\partial^2 \psi}{\partial x \partial y} & \frac{\partial^2 \psi}{\partial y^2} \end{bmatrix}^T \tag{3}$$

Where, m_i and n_i are various material constants. For a symmetric laminated composite, the values of the coefficients are obtained as $m_1 = m_3 = n_2 = 0$, $m_2 = 1$, $n_1 = \frac{-A_{11}}{A_{12}+A_{66}}$ and $n_3 = \frac{-A_{66}}{A_{12}+A_{66}}$. The values of the coefficients are determined in such way that with the definition of $\psi(x, y)$, the first equilibrium equation (2a) is identically satisfied [7]. Therefore, ψ has to satisfy the second equilibrium equation (2b) only. Expressing equation (2b) in terms of the function $\psi(x, y)$, the single governing differential equation of equilibrium for the symmetric laminated composites is obtained as follows:

$$\frac{\partial^4 \psi}{\partial x^4} + \left(\frac{A_{22}}{A_{66}} - \frac{A_{12}^2}{A_{11}A_{66}} - \frac{2A_{12}}{A_{11}} \right) \frac{\partial^4 \psi}{\partial x^2 \partial y^2} + \frac{A_{22}}{A_{11}} \frac{\partial^4 \psi}{\partial y^4} = 0 \tag{4}$$

The explicit expressions of the displacement components in terms of the function are

$$\begin{bmatrix} u_x \\ u_y \end{bmatrix} = \begin{bmatrix} 0 & 1 & 0 \\ \frac{-A_{11}}{A_{12}+A_{66}} & 0 & \frac{-A_{66}}{A_{12}+A_{66}} \end{bmatrix} \begin{bmatrix} \frac{\partial^2\psi}{\partial x^2} & \frac{\partial^2\psi}{\partial x\partial y} & \frac{\partial^2\psi}{\partial y^2} \end{bmatrix}^T \tag{5}$$

From equation (1) and (5), the corresponding expressions of stress components in terms of the function, $\psi(x, y)$, are,

$$\begin{bmatrix} \sigma_{xx} \\ \sigma_{yy} \\ \sigma_{xy} \end{bmatrix} = \frac{1}{h(A_{12}+A_{66})} \begin{bmatrix} 0 & A_{11}A_{66} & 0 & -A_{12}A_{66} \\ 0 & A_{12}^2 + A_{11}A_{66} - A_{11}A_{22} & 0 & -A_{22}A_{66} \\ -A_{11}A_{66} & 0 & A_{12}A_{66} & 0 \end{bmatrix} \begin{bmatrix} \frac{\partial^3\psi}{\partial x^3} & \frac{\partial^3\psi}{\partial x^2\partial y} & \frac{\partial^3\psi}{\partial x\partial y^2} & \frac{\partial^3\psi}{\partial y^3} \end{bmatrix}^T \tag{6}$$

Stresses at individual plies of the laminate are calculated from the global mid-plane strain (ε_{ij}) and the respective transformed reduced stiffness matrix, $\left[\overline{Q}_{ij}\right]$ of the ply [9].

A uniform rectangular mesh-network is used to discretize the plate, which includes an imaginary boundary, immediate exterior neighbor to the physical boundary of the plate. Finite-difference method is used to replace the differential equations associated with the equilibrium and boundary conditions by their corresponding difference equations. The order of local truncation error has been kept the same ($O(h^2)$) for all the expressions developed. Different versions of finite-difference expressions for each of the boundary conditions are developed by adopting various combinations of forward, backward and central difference schemes, for nodal points on different segments of the boundary. Finally, the nodal solutions of the function $\psi(x, y)$ are used to calculate the required displacement, strain and stress fields of the plate through the respective difference equations.

3. Geometry and loading of the laminated plate

The geometry and loading of a locally restrained laminated composite plate subjected to a uniform bi-axial compression is shown in Fig. 1. Two different composite plates of angle-ply and cross-ply laminates are considered for the present analysis. The length, width and thickness of the plate are represented by a, b and h, respectively. Both the plates are composed of eight plies of graphite reinforced aluminum matrix composite of identical thickness, the stacking sequences of which are $[45/-45/45/-45]_s$ and $[0/90/0/90]_s$, respectively. The opposing parallel surfaces of the plate are subjected to uniform compression of identical intensity. The four corner regions of the plate are assumed to be rigidly fixed to simulate the condition of tag welding.

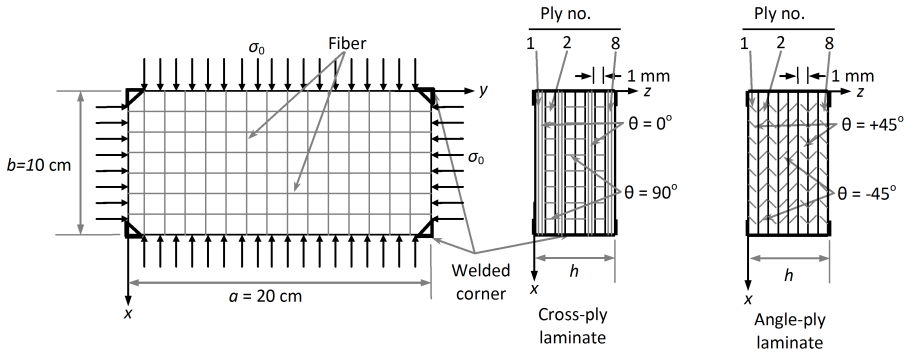

Fig. 1: Geometry, loading and fiber orientation of the laminated plate.

4. Temperature dependent mechanical properties of the composite

The composite material under investigation was composed of Thornel P100 graphite fibers embedded in a 6061 aluminum matrix. It was manufactured by an infiltration/liquid phase hot pressing process. The consolidated panels

were 0.305 by 0.305 m wide and 1.02 mm thick. The average fibre volume fraction of the panels was 46.6%. All mechanical tests were performed on specimens prepared from the above panels. The low thermal expansion coefficient of the graphite fibers in the longitudinal direction along with the high Young's modulus of the P100 fibre make this composite attractive for application requiring a high degree of dimensional stability in a wide temperature range. Tests were performed at four different temperature conditions, which are -101^o, 24^o (room condition), 121^o, and 260^oC [1]. The effective mechanical properties of P100/6061 Gr-Al composite obtained at different working temperatures are listed in Table 1.

Table 1: Mechanical properties of on-axis P100/6061 graphite/Aluminum specimens at different temperatures.

Composite	Property	Symbol	-101^oC	24^oC	121^oC	260^oC
Graphite-Aluminum	Elastic modulus along the fiber direction	E_1 (GPa)	379.9	402.6	392.3	292.9
	Elastic modulus perpendicular to the fiber direction	E_2 (GPa)	29.6	24.1	28.3	24.1
	Shear modulus	G_{12} (GPa)	23.78	19.02	20.89	17.65
	Major Poisson's ratio	ν_{12}	0.328	0.291	0.297	0.294

5. Results and discussions

Mechanical behavior of the laminated plates under a uniform bi-axial compression is investigated for four different working temperatures, which are -101^o, 24^o, 121^o, and 260^oC. The plate is kept fixed by local restraints at its four corners, in which the area of each restrained region is only 0.16% of the total plate area. The magnitude of loading intensity is assumed to be $\sigma_0 = 3$ MPa for both the laminates. The thickness of individual plies is kept constant to 1.0 mm. A (53×53) finite-difference mesh-network is used to model the laminated plate of aspect ratio, $a/b = 2$.

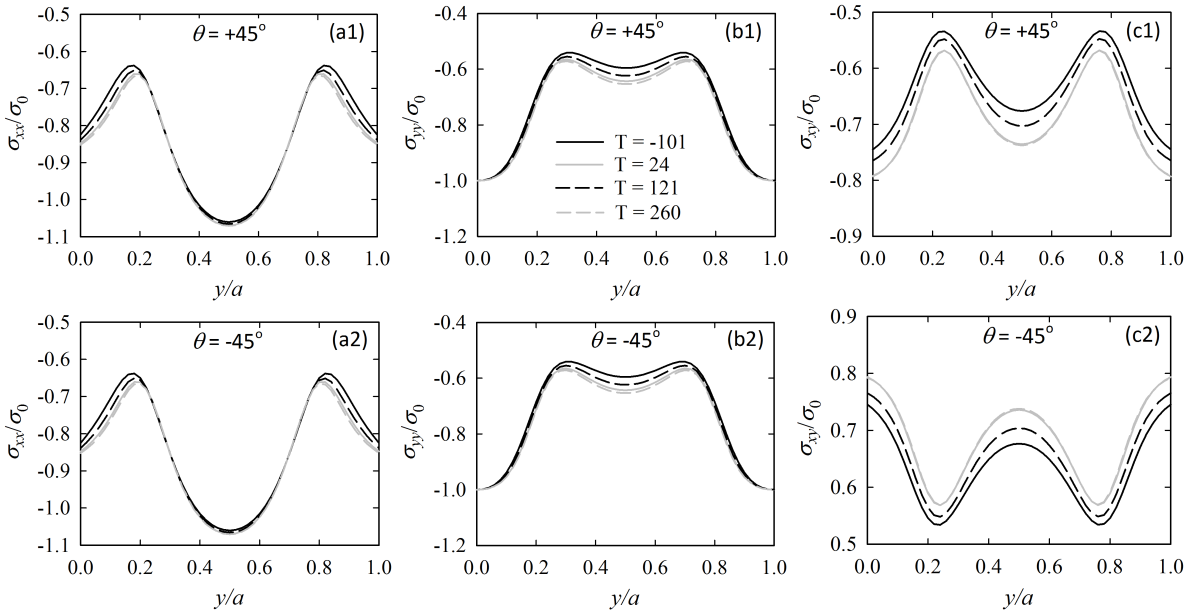

Fig. 2: Distribution of stress components along the mid-section of the angle-ply laminated plate as a function of fiber orientation and temperature.

Figure 2 describes the effect of the variation of temperature as well as fiber orientation of angle-ply laminate on the distribution of the global stresses along the mid-section $(x/b = 0.5)$ of the plates. As appears from Fig. 2, both the magnitude and nature of variation of (σ_{xx}/σ_0) are found to be very similar for all the temperature as well as plies of the

angle-ply laminate. A V-shaped distribution of the stresses is encountered, which varies within $0.6 \leq \sigma_{xx}/\sigma_0 \leq 1.1$. For the case of axial stress component, a symmetric M-shaped distribution of stresses is encountered for both the plies. For the case of shear stress, distributions in individual plies are identified to be mirror image of each other, in which the stress level, in general, is found to increase with the increase of temperature. Maximum magnitude of the stress is found at occur at the left and right boundaries of the plate.

Figure 3 shows the distributions of normalized stress components at the the mid-lateral section ($x/b = 0.5$) of the cross-ply laminated plates under bi-axial loading. For the case of lateral stress, both plies assume a flat U-shaped distribution at all temperature levels. Magnitude of stresses is found to be nearly 10 times higher for $\theta = 0^o$–ply compared to that of $\theta = 90^o$–ply. The general trend of distributions for $\theta = 90^o$–ply shows that lateral stress decreases with the increase of exposure temperature. At room temperature condition, the corresponding distribution becomes very close to that at 260^oC, which is however well consistent with the corresponding material properties (Table 1). For the case of axial stress, distributions are found to be different for different plies of the cross-ply laminate, in which stress level is much higher for $\theta = 90^o$–ply compared to that of $\theta = 0^o$–ply. Temperature dependency of stresses is more prominent in cross-ply laminate; in general, with the increase of temperature, stress level decreases for the $\theta = 0^o$–ply, however, an opposite phenomenon is observed for $\theta = 90^o$–ply. Axial stresses are found to assume maximum values at the lateral ends of the plate. On the other hand, the mid-sections of both the plies of the cross-ply laminate are found to be completely free from shearing stresses, which is because of the symmetry of the problem.

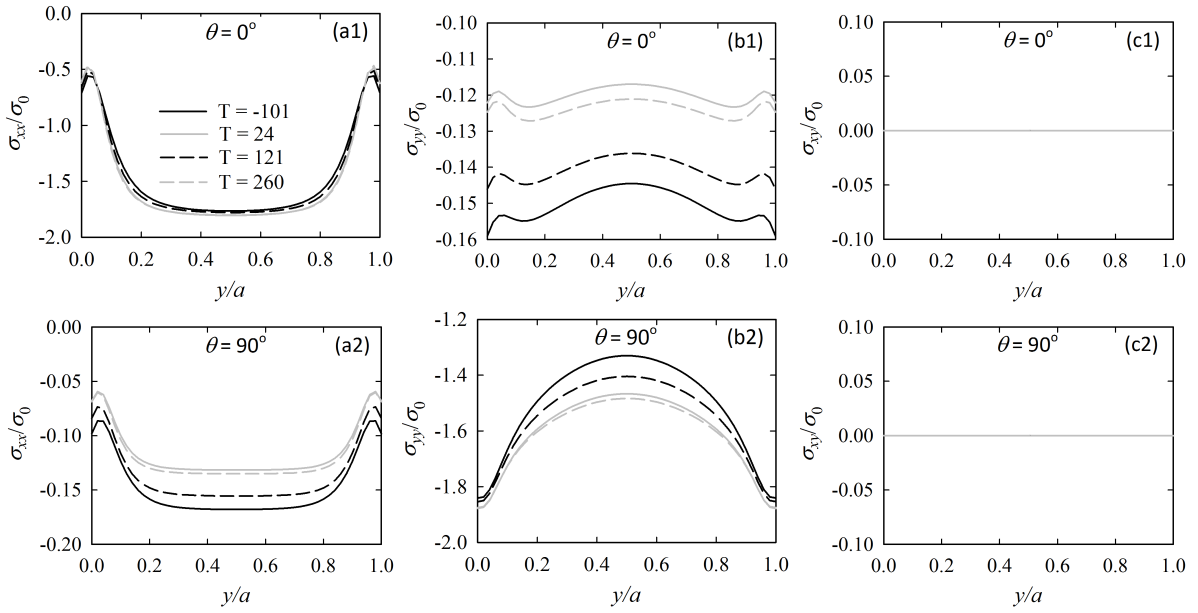

Fig. 3: Distribution of stress components along the mid-section of the cross-ply laminated plate as a function of fiber orientation and temperature.

Figure 4 shows the deformed shapes of the plates obtained at 121^oC together with their un-deformed shapes. The overall deformation pattern of the plate is found to be in good agreement with the physical model of the problem, which verifies the appropriateness of the present modeling. Axial deformation of the angle-ply laminate is slightly higher than that of cross-ply laminate, whereas lateral deformation is, to some extent, higher for the case of cross-ply laminate.

Table 2 lists the critical local stresses developed at the corner restrained regions of the two laminated plates. Local stresses at the restrained sections are found to be higher than the global stresses in both the laminates. Because of the symmetry of the problem, identical stress concentrations are encountered at all the four restrained regions. The cross-ply laminate is identified to be more critical in terms of local stresses.

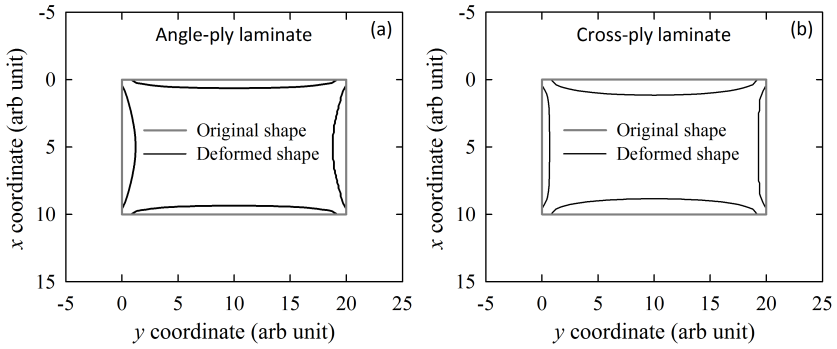

Fig. 4: Deformed shapes of the plate under bi-axial loading (magnification factor, ×1000): (a) Angle-ply, (b) Cross-ply laminate.

Table 2: Local stresses at the restrained corner region of the laminated plates at different temperature.

Section	Normalized stress	Angle-ply laminate				Cross-ply laminate			
		$T = -101^o$	$T = 24^o$	$T = 121^o$	$T = 260^o$	$T = -101^o$	$T = 24^o$	$T = 121^o$	$T = 260^o$
Corner	σ_{xx}/σ_0	1.112	1.017	1.058	0.996	0.674	0.539	0.591	0.511
	σ_{yy}/σ_0	2.279	1.720	1.935	1.614	7.349	7.267	7.297	7.209
	σ_{xy}/σ_0	2.282	2.213	2.248	2.194	2.651	2.373	2.472	2.281

6. Conclusions

Temperature-dependent mechanical behavior of a locally restrained graphite/aluminum laminated plate is investigated under a uniform bi-axial compression. The deformed shapes as well as global stresses are found to be influenced primarily by the ply angle and, to some extent, by the working temperature. The cross-ply laminated plate is identified to be more critical than angle-ply laminate in terms of both local and global stresses. Local stresses are found to be much higher than global ones, which are however highly localized only at the restrained regions.

References

[1] T. Frujita, M.J. Pindera, C.T. Herakovich, Temperature dependent tensile and shear Response of P100/6061 Graphite-Aluminum, in: J.M. Kennedy, H.H. Moller and W.S. Johnson (Eds.), Thermal and Mechanical Behavior of Metal Matrix and Ceramic Matrix Composites, ASTM STP 1080, Philadelphia, 1990, pp. 165–182.

[2] J.M. Lifshitz, Strain rate, temperature and humidity influences on strength, moduli of graphite/epoxy composite, NASA, Ames Research Center, Moffett Field, California, 1981.

[3] I. Dutta, D.L. Bourell, A theoretical and experimental study of Al alloy 6061-SiC metal matrix composite to identify the operative mechanism for accelerated aging, Materials Science and Engineering: A 112 (1989) 67–77

[4] G. Agarwal, A. Patnaik, R. K. Sharma, Thermo-mechanical properties of silicon carbide-filled chopped glass fiber-reinforced epoxy composites, International Journal of Advanced Structural Engineering 5 (2013) 1–8.

[5] D.L. Majid, E.J. Abdullah, N.F. Harun, G.Y. Lim, B.T.H.T. Baharudin, Effect of Fiber Orientation on the Structural Response of a Smart Composite Structure, Procedia Engineering 50 (2012) 445–452

[6] T. Vincent, T. Ozbakkaloglu, Influence of fiber orientation and specimen end condition on axial compressive behavior of FRP-confined concrete, Construction and Building Materials 47 (2013) 814–826

[7] S.R. Ahmed, M.Z. Hossain, M. W. Uddin, A general mathematical formulation for finite-difference solution of mixed-boundary-value problems of anisotropic materials, Computers & Structures 83 (2005) 35–51

[8] S.R. Ahmed, A.A. Mamun, P. Modak, Analysis of stresses in a simply supported composite beam with stiffened lateral ends using displacement-potential field, International Journal of Mechanical Sciences 78 (2014) 140–153

[9] R.M. Jones, Mechanics of Composite Materials, McGraw-Hill, New York, 1975

[10] S. Timoshenko, V.N. Goodier, Theory of Elasticity, third ed., McGraw-Hill, New York, 1979.